# Hybrid Visible Light and Power Line Communication for Indoor Multiuser Downlink

Hao Ma[1], Lutz Lampe[1] and Steve Hranilovic[2]
[1] Department of Electrical and Computer Engineering, University of British Columbia, Vancouver, Canada
Email: Lampe@ece.ubc.ca
[2] Department of Electrical and Computer Engineering, McMaster University
Email: hranilovic@mcmaster.ca

***Abstract*—Visible light communication (VLC) turns indoor light-emitting diode (LED)-based illumination devices into high-speed network portals that, for example, operate in tandem with existing Wi-Fi networks. Since in this scenario multiple VLC-equipped luminaires would serve overlapping service areas, we suggest the use of power line communication (PLC) to coordinate and provide data to the VLC transmitters. In particular, in this paper, we propose a hybrid VLC-PLC (HVP) system architecture for the indoor downlink transmission and present the analytical framework for the data rate analysis of the HVP system. In our solution, spatial optical OFDM (SO-OFDM) is applied across multiple luminaires, for which we propose several subcarrier allocation schemes to exploit the frequency selectivity of the VLC and PLC channels. Different possible and meaningful variations of the HVP system, including the choice of optical OFDM transmission, relay and multiple access schemes, are investigated and compared. The numerical results establish achievable rates for relevant communication scenarios and highlight the advantages of the proposed subcarrier allocation scheme in terms of rate and reduced peak power of optical OFDM signals.**

## I. Introduction

The lighting industry is undergoing a major technology transition as energy-efficient light-emitting diode (LED) illumination devices are replacing both incandescent and fluorescent light bulbs. The long lifetime of LED luminaires is encouraging lighting companies to adjust their business model from lighting equipment manufacturers to light-as-a-service providers. Visible light communication (VLC) technology is a potential enabler in this business transition. VLC can utilize LED lighting fixtures as transmission devices and information can be conveyed through varying the illumination intensity of the light carrier. This symbiotic relationship with lighting systems makes VLC easily deployable wherever LED lighting has been adopted, including in electromagnetic interference sensitive areas like hospitals. As lighting companies explore opportunities to add value to lighting systems, VLC technology can turn LED luminaires into network portals especially facilitating the downlink of network operator services for indoor users. These portals would not necessarily substitute but more likely complement existing radio-frequency (RF) solutions such as WiFi systems to provide ubiquitous and high-speed coverage [2]–[4].

This work has been supported by the Natural Sciences and Engineering Research Council of Canada (NSERC). This work has been presented in part at the IEEE International Symposium on Circuits and Systems (ISCAS), Montreal, Canada, May 2016 [1].

Though VLC outperforms RF communication in terms of availability of unlicensed spectrum and spatial reuse, it does not fully avoid interference inherent to wireless systems. Although visible light does not penetrate opaque walls, multiple LED luminaires usually exist in close proximity inside a room to ensure a uniform illumination level. The resulting overlap of their emissions leads to interference of VLC signals from neighboring LED luminaires, which in turn can seriously degrade VLC system performance [5]. To exploit the overlapping coverage, [5]–[8] proposed the coordination of different LED luminaires through a backbone network, and [5] shows that coordinated VLC systems can improve the signal-to-interference-plus-noise ratio (SINR) at the user up to 30 dB compared to an uncoordinated VLC system. Candidates for the backbone network are Ethernet and low-voltage power line communication (PLC) links. PLC seems a more pragmatic choice given that it is possible to leverage existing infrastructure already in place at each luminaire [9], [10]. Furthermore, data rates of modern broadband PLC systems are on the order of up to hundreds of Mbps or even Gbps and thus sufficient to support indoor data links, as also demonstrated for PLC-WiFi systems [11], [12]. We note that the integration of VLC and PLC is not new, e.g., [13], [14]. However, the coordinating role of PLC for VLC in such a hybrid VLC-PLC (HVP) system, in which the PLC modem is connected to the outside access network and acts not only as a data source for VLC luminaires but also as a central controller for multiple luminaires, has only been presented recently [6], [7], [15].

Backbone PLC systems are typically broadband in nature and employ orthogonal frequency-division multiplexing (OFDM) [16]. OFDM has also been studied for VLC transmission, e.g., [17], [18], to deal with the frequency selectivity of the VLC channel. One of the challenges for an optical OFDM implementation is the high peak-to-average power ratio (PAPR) of the time-domain signal. It leads to signal distortions due to the non-negativity constraint for the optical time-domain signal and a reduced energy-efficiency for practical LED drivers with limited dynamic range. To alleviate the PAPR problem, recently [19] designed and analyzed spatial-optical OFDM (SO-OFDM) schemes, in which (possibly overlapping) subsets of OFDM subcarriers are transmitted over subsets of LEDs of a luminaire, and the entire OFDM signal results from spatial summing. In the extreme case of a single subcarrier per LED, this leads to a PAPR of only 3 dB.

In this work, we propose an HVP system for indoor downlink optical wireless access utilizing the SO-OFDM technique. Compared to traditional VLC-PLC integration, our system enables end-to-end use of OFDM modulation, alleviates the high PAPR problem of OFDM for LED transmitters, and enables the cooperation of multiple spatially distributed luminaires to overcome inter-luminaire interference and increase robustness against possible signal obstruction from a single luminaire. To this end, we make the following contributions.

1) We develop the HVP system together with an analytical framework for its achievable rate. Inspired by cooperative transmission techniques widely studied in the RF domain, we consider the HVP system as a relay-assisted two-hop communication system without a direct link between the source and the destination. The LED luminaires act as full-duplex relays (transmit and receive signals at the same time) and retransmit the received PLC signal to the user via VLC. Considering the channel characteristics of PLC and VLC and the fact that VLC uses intensity modulation, i.e., the transmitted signal must be non-negative and operates under a peak amplitude constraint, we derive expressions for the rate that can be supported by the HVP system.
2) We generalize SO-OFDM proposed in [19] by considering the joint subcarrier allocation (SA) among multiple spatially distributed LED luminaires, and we propose several SA schemes for this SO-OFDM HVP system to exploit the frequency diversity of PLC and VLC channels, and multi-user diversity in case of multiple users. This includes a subcarrier pairing (SP) method that adaptively matches between incoming and outgoing subcarriers at the LED luminaire to account for the frequency selectivity of the two channels.
3) For multi-user HVP systems, the SA schemes are developed for two possible multiple access schemes: OFDM time-division multiple access (OFDM-TDMA) and orthogonal frequency-division multiple access (OFDMA). SA of multi-user HVP systems is a non-trivial task due to the coupling of subcarrier pairing, relay selection and user selection, and the limited number of subcarriers per LED luminaire set by SO-OFDM. To reduce the computational complexity of SA, we investigate the performance of chunk-based SA [20] and propose several suboptimal polynomial-time SA algorithms. We note that the contribution of our work is not dependent on any specific OFDM signal format employed by the VLC link. We adopt two variations of OFDM signal formats as the VLC multicarrier solutions in this paper due to their popularity. However, the proposed optimization framework can be easily extended to any other OFDM signal formats in SO-OFDM-based HVP systems.

The remainder of the paper is organized as follows. In Section II, we introduce the SO-OFDM-based HVP system, and present the channel and noise models for the PLC and VLC links. In Section III, different optical OFDM formats and relay protocols are investigated for the HVP system, and the corresponding achievable rate expressions are presented. In Section IV, computationally efficient SA algorithms, with and without SP, are proposed for the two multi-access schemes. Simulation results for different variations of HVP systems are presented and discussed in Section V. Finally, the conclusions are drawn in Section VI.

The following notations are used in this paper. $|\cdot|$ represents the cardinality operator. $\mathbb{E}[\cdot]$ denotes statistical expectation. The $^*$ superscript denotes the complex conjugate, and $\boldsymbol{I}_{n\times n}$ is the $n \times n$ identity matrix.

## II. System Model

### A. Problem Scenario

We propose an SO-OFDM-based HVP system for downlink transmission to $N_{\mathrm{U}}$ users located in the same room and served via the cooperation of $N_{\mathrm{L}}$ LED luminaires, and each luminaire consists of $N_{\mathrm{E}}$ LEDs. Fig. 1 illustrates the system structure showing a single user. The power line acts as the backbone network that feeds data to and coordinates cooperation among the multiple VLC-equipped LED luminaires, which in turn operate as full-duplex relays which process the received PLC signal and forward it via VLC to indoor users. Applying SO-OFDM across multiple luminaires, each luminaire only emits a subset of the data symbols from the received PLC OFDM signal. The VLC signals from multiple LED luminaires superpose at the photo-diode detectors of the users, where a conventional OFDM receiver can be used to decode the information. To achieve this, accurate time and frequency synchronization is required for the VLC hop. Since both VLC and PLC OFDM are baseband modulated, carrier frequency offset is absent and only timing needs to be taken care of. To resolve the time synchronization problem resulting from the time difference of arrivals (TDOA) of users' signal at the luminaires, we can ensure that the cyclic prefix length of the OFDM symbol is longer than the TDOA. Further considering the fact that the line-of-sight (LOS) link plays the major role in VLC systems [21], and the inter-luminaire distances between VLC transmitters in the indoor environment are relatively small, the situation here is relatively simpler compared to Coordinated Multi-Point (CoMP) systems with RF implementation [22]. In the rest of the paper, we assume VLC transmitters are perfectly synchronized. For the HVP uplink, both optical and RF uplinks are potential candidates. An optical uplink suffers from problems like energy inefficiency and device glare, and the required LOS link between the device and the fixed uplink receiver can be easily lost due to user mobility and change in device orientation [23]. Thus an RF uplink is preferred considering that most places are RF-insensitive. One choice is a WiFi uplink, because most mobile devices have WiFi radio pre-installed already. The integration of WiFi uplink with VLC has been discussed in a number of research works in the literature, e.g., [2], [23]–[25]. The WiFi uplink, for the HVP system specifically, can be implemented through a PLC-WiFi integrated modem (which could act as the coordinator point), as illustrated in Fig. 1. Such an uplink would provide the channel state information (CSI) about the VLC links to the coordinator point for system optimization.

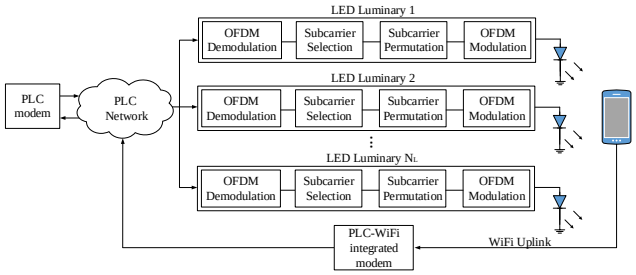


Fig. 1. Block diagram of the HVP system.

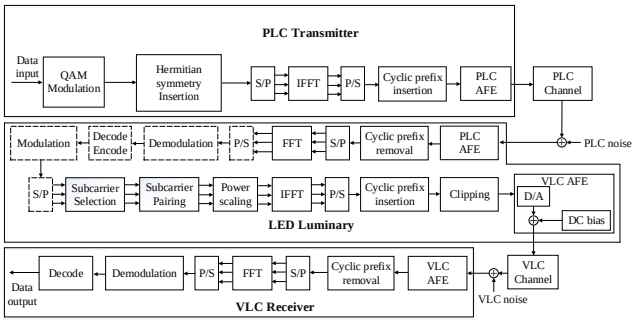


Fig. 2. Detailed block diagram of the SO-OFDM HVP downlink system for one luminaire and one user. Blocks with dashed lines are not present in LED luminaires operating in amplify-and-forward mode.

### *B. Transmitter and Receiver Model*

Fig. 2 shows a detailed block diagram of the SO-OFDM HVP system with respect to a specific luminaire relay. We note that the baseband OFDM signals transmitted over the PLC and VLC links satisfy the Hermitian symmetry property in the frequency domain, and in the following, we will only describe the processing for the independent information-carrying subcarrier sets ($\mathcal{P}_{\text{info}}$ and $\mathcal{V}_{\text{info}}$ in Section III).

In the PLC hop, the PLC modem broadcasts the same wideband OFDM signal to every LED luminaire containing $N_{\text{p}}$ independent information-carrying subcarriers. In the VLC hop, SO-OFDM is applied, and the $k_{\text{th}}$ luminaire re-modulates $N_k$ of the received PLC data symbols onto $N_k$ of $N_{\text{v}}$ available VLC subcarriers. The $N_{\text{v}} - N_k$ unused subcarriers are set to zero. The subcarrier subsets across different luminaires are disjoint and we have $\sum_{k=1}^{N_{\text{L}}} N_k = N_{\text{p}}$. At each LED luminaire, we consider a subcarrier pairing approach which adaptively matches incoming with outgoing subcarriers to fully exploit the frequency diversity of both PLC and VLC channels. The number of subcarriers $N_k$ and thus subcarrier pairs assigned to the $k_{\text{th}}$ luminaire cannot exceed an upper limit in order to limit the PAPR of the OFDM signal at each LED luminaire.

We consider two operating modes for the LED luminaire relay, namely amplify-and-forward (AF) and decode-and-forward (DF). An AF-mode luminaire relay demodulates the PLC signal, scales the selected subcarrier signals, and re-modulates them applying subcarrier pairing. In addition to this, a DF-mode relay also decodes the received signal. Only if decoding is deemed successful, based on an outer error-detection code, the DF-mode relay will re-encode and re-modulate the data, and then forward it to the destination.

At the user side, the VLC analog front-end (AFE) consists of a photo-diode detector to convert the optical to an electrical received signal and an AC coupler to remove the DC signal component, which is responsible for the primary illumination function of the LED luminaires. This is followed by a conventional OFDM receiver.

### *C. Channel and Noise Model*

*1) Power Line Communication:* To faithfully model the signal transfer over the low-voltage power line network, we apply the bottom-up approach based on transmission-line theory as presented in [26], [27] and implemented in a simulator in [28], which leads to a distinctive PLC channel for each LED luminaire based on the cable characteristics of its corresponding power line branch. The noise in PLC systems consists of colored background noise, narrowband disturbance, and impulsive noise [16]. We model the first two terms through the combined power spectral density (PSD) of the shape as in [29, Eq. (4)], as also adopted in the IEEE 1901 standard [30, Annex F.3.5.2]. Impulse noise is modeled as a non-stationary random process. For the purpose of mathematical tractability, we disregard the impulse noise in the rate optimization. This is justified as the impulse noise events occur with relatively low probability (see. e.g. [31]) and if significant lead to outage events. Furthermore, one of the major components of impulse noise in the low-voltage power line is the random aperiodic impulse noise. In this case, rate optimization considering the aperiodic noise for the purpose of adaptive transmission is ineffective. Note that in all the numerical results presented in Section V, we will consider the impulse noise for the purpose of simulation accuracy, and we apply the two-state approximation as in [32, Eq. (19)] to calculate the achievable rate. To enable the reproducibility of the numerical results, we have made the PLC noise simulator available online [33].

*2) Visible Light Communication:* The VLC channel is frequency selective due to the low-pass characteristics of the LED emission and the multipath dispersion of the VLC signal. The latter starts to play a role when the bandwidth of the transmitted signal exceeds 20 MHz [34], which is the case for the considered HVP system. In this paper, we take both the line-of-sight (LOS) link and non-line-of-sight (NLOS) link (reflections) into consideration for the VLC channel modeling. We assume that propagation from either the LED source or a reflection point on the walls follows the Lambertian radiation pattern. The channel gain $h$ between the receiver (the user or a reflection point on the walls) and the light source (the LED source or a reflection point on the walls) can then be expressed as [35]

$$h = \frac{(m+1)s\gamma\kappa^2 A_{\text{PD}}}{2\pi D^2 \sin^2(\psi_c)} \cos^m(\phi)\cos(\psi)\mathbb{I}_{\mathcal{A}}(\psi)\ , \qquad (1)$$

where $m$ is the Lambertian order and specifies the transmit beam divergence, $s$ is the receiver responsivity, $\gamma$ is the

conversion factor of the light source, $\kappa$ is the concentrator refractive index, $D$ is the distance between the receiver and the light source, $\psi_c$ is the width of the field of view (FOV) at the receiver, $A_{\rm PD}$ is the area of photodetector, $\psi$ is the angle of incidence at which the light is received relative to the normal vector of the receiver plane, $\phi$ is the angle of irradiance at which the light is emitted relative to the normal vector of the transmitter plane. Furthermore, $\mathbb{I}_{\mathcal{A}}(\psi)$ denotes the indicator function, and $\mathcal{A} = \{\psi |\ 0 \leq \psi \leq \psi_c\}$. Based on (1), we apply the modified Monte Carlo method presented in [36] to obtain the frequency-domain channel gain $H_{\rm CL}(f)$ in our simulations, and our source code written in MATLAB is available at [37]. The first three reflections are taken into account as they carry most of the VLC signal power. Together with the frequency response for the LED emissions which can be approximated by [38]

$$H_{\rm LED}(f) = \frac{1}{1 + j\frac{f}{f_{\rm LED}}}\ , \tag{2}$$

with $f_{\rm LED}$ representing the 3 dB cutoff frequency of the LED low-pass characteristics, the overall VLC channel gain can be expressed as

$$H_{\rm v}(f) = H_{\rm LED}(f) H_{\rm CL}(f). \tag{3}$$

The noise in VLC systems comprises shot noise, which is induced by ambient light, and thermal noise. The total VLC noise can be modeled as a zero-mean Gaussian random variable with variance [21]

$$\sigma^2_{\rm vn} = 2e{\rm W}_{\rm v}(I_{\rm rp} + I_{\rm bg} I_2) + \sigma^2_{\rm th}\ , \tag{4}$$

where $e$ is the elementary charge, ${\rm W}_{\rm v}$ is the VLC system bandwidth, $I_{\rm bg}$ is background current, $I_2$ is the noise bandwidth factor (second Personick integral [39]), $I_{\rm rp}$ is the average current of the received signal, and $\sigma^2_{\rm th}$ is the thermal-noise variance.

## III. Rate Analysis of the HVP System

In this section, we derive the expressions for the achievable rates for downlink transmission with the HVP system using different relaying strategies. More specifically, we consider the rate associated with a single OFDM subcarrier pair of the PLC-VLC link to a single user. Since different subcarriers are orthogonal and since users are multiplexed over orthogonal subcarriers or time slots, rate expressions of the total HVP system follow then immediately.

### A. Signal at the PLC Hop

The baseband PLC OFDM signal uses the set $\mathcal{P}_{\text{info}}$ of information-carrying subcarriers, where $|\mathcal{P}_{\text{info}}| = N_{\rm p}$. Denoting the PLC frequency-domain transmitted symbol at subcarrier $l$ as $X_{\rm p}(l)$, and with the usual assumptions about sufficient cyclic-prefix length, synchronization, and channel time-invariance, the PLC frequency-domain signal $Y^k_{\rm p}(l)$ at subcarrier $l$ received by the $k_{\rm th}$ LED luminaire can be expressed as

$$Y^k_{\rm p}(l) = H^k_{\rm p}(l) X_{\rm p}(l) + N^k_{\rm p}(l)\ , \tag{5}$$

where $H^k_{\rm p}(l)$ and $N^k_{\rm p}(l)$ are the PLC channel gain and noise for subcarrier $l$ at the $k_{\rm th}$ LED luminaire, respectively. The corresponding signal-to-noise ratio (SNR) is

$${\rm SNR}^k_{\rm p}(l) = \frac{\left|H^k_{\rm p}(l)\right|^2 \sigma^2_{\rm p}}{\sigma^2_{{\rm pn},k}(l)}, \tag{6}$$

where $\sigma^2_{\rm p} = \mathbb{E}\big[|X_{\rm p}(l)|^2\big]$ and $\sigma^2_{{\rm pn},k}(l) = \mathbb{E}\left[\left|N^k_{\rm p}(l)\right|^2\right]$.

### B. Signal at the VLC Hop

The $k_{\rm th}$ VLC transmitter modulates $N_k$ subcarriers from the set $\mathcal{V}_{\text{info}}$ of active information-carrying subcarriers, and $|\mathcal{V}_{\text{info}}| = N_{\rm v}$. Denoting the frequency-domain transmitted symbol over subcarrier $l$ as $X^k_{\rm v}(l)$ and the size of the discrete Fourier transform applied for VLC as $N^{\rm v}_{\rm fft}$, the time-domain samples at each element of the $k_{\rm th}$ luminaire can be expressed as

$$x^k_{\rm v,info}(n) = \frac{1}{\sqrt{N^{\rm v}_{\rm fft}}} \sum_{l=0}^{N^{\rm v}_{\rm fft}-1} X^k_{\rm v}(l) {\rm exp}\left(\frac{j2\pi nl}{N^{\rm v}_{\rm fft}}\right)\ , \tag{7}$$

where Hermitian symmetry $X^k_{\rm v}(l) = \left(X^k_{\rm v}(N^{\rm v}_{\rm fft} - l)\right)^*$ holds, and only $2N_k$ out of $N^{\rm v}_{\rm fft}$ $X^k_{\rm v}(l)$ are non-zero due to SO-OFDM (see Section II-B). The signal $x^k_{\rm v,info}(n)$ is used to modulate the intensity of the LED luminaire. To make the signal compatible with the IM/DD channel, in the following we consider both DC-biased optical OFDM (DCO-OFDM) and asymmetrically clipped optical OFDM (ACO-OFDM), which are the two popular forms of intensity-modulated optical OFDM [40], [41].

Since an LED as a transmitter has a limited dynamic range, the time-domain OFDM signal may be clipped due to a high PAPR [42]. Let $I_{\rm min}$ and $I_{\rm max}$ represent the lower and upper bound of the LED forward current, respectively, and $I_{\rm DC}$ be the DC bias current. Then, the clipped signal can be expressed as

$$x^k_{\rm v,clip}(n) = F_{\rm CLIP}(x^k_{\rm v,info}(n))\ , \tag{8}$$

where [43]

$$F_{\rm CLIP}(x) = \begin{cases} b & x \leq b\ , \\ t & x \geq t\ , \\ x & \text{otherwise}\ , \end{cases} \tag{9}$$

and $t = I_{\rm max} - I_{\rm DC}$, $b = I_{\rm min} - I_{\rm DC}$ for DCO-OFDM, and $t = I_{\rm max} - I_{\rm DC}$, $b = \max(I_{\rm min} - I_{\rm DC}, 0)$ for ACO-OFDM. Neglecting possible differences among LEDs located at the same luminaire, we obtain the equivalent transmitted signal of the $k_{\rm th}$ LED luminaire as

$$x^k_{\rm v,sum}(n) = N_{\rm E}\left(x^k_{\rm v,clip}(n) + I_{\rm DC}\right)\ . \tag{10}$$

We note that the level of the bias current, which together with clipping ensures the non-negativity of the transmit signal, is determined by the illumination requirement on the luminaire.

To proceed with formulating the received signal after the VLC link, we need to distinguish between the OFDM modalities used at the VLC transmitter (DCO-OFDM or ACO-OFDM) and the relaying methods (DF or AF) to obtain $X^k_{\rm v}(l)$. This is done in the next subsection, where we derive

the associated expressions for achievable rates for a single subcarrier pair of the HVP system.

### C. Achievable Rate Expression for Each Subcarrier Pair

*1) DCO-OFDM:* For DCO-OFDM, $\mathcal{V}_{\text{info}} = \{1, 2, \ldots, N_{\text{v}}\}$. According to Bussgang's theorem [44], the clipped signal at the $k_{\text{th}}$ luminaire can be modeled as an attenuation of the original signal plus a non-Gaussian uncorrelated noise component [45]:

$$x^k_{\text{v,clip}}(n) = A^k x^k_{\text{v,info}}(n) + n^k_{\text{c}}(n) \ , \tag{11}$$

where $n^k_{\text{c}}(n)$ is the non-Gaussian clipping noise term with variance $\sigma^2_{\text{clip},k}$ and $A^k$ is the attenuation factor. Given the electrical power of the VLC signal $P^k_{\text{v}} = \sum_{l=0}^{N^{\text{v}}_{\text{fft}}-1} \mathbb{E}\left[|X^k_{\text{v}}(l)|^2\right]/N^{\text{v}}_{\text{fft}}$ and the constants from the clipping function (9), and defining the normalized clipping levels $b^k = b/\sqrt{P^k_{\text{v}}}$ and $t^k = t/\sqrt{P^k_{\text{v}}}$, we have [43], [46]

$$A^k = Q\left(b^k\right) - Q\left(t^k\right) \ , \tag{12}$$

and

$$\begin{aligned}\sigma^2_{\text{clip},k} =& P^k_{\text{v}}\Big(A^k - (A^k)^2 + \left(1 - Q(b^k)\right)(b^k)^2 + Q(t^k)(t^k)^2 \\ &- \left(\phi(b^k) - \phi(t^k) + \left(1 - Q(b^k)\right) b^k + Q(t^k)t^k\right)^2 \\ &+ \phi(b^k)b^k - \phi(t^k)t^k\Big) \ ,\end{aligned} \tag{13}$$

where $Q(\cdot)$ and $\phi(\cdot)$ are the tail probability function and the probability density function of the standard normal distribution.

Substituting (11) into (10) gives the output signal at the $k_{\text{th}}$ LED luminaire as

$$x^k_{\text{v,sum}}(n) = N_{\text{E}} A^k x^k_{\text{v,info}}(n) + N_{\text{E}} n^k_{\text{c}}(n) + N_{\text{E}} I_{\text{DC}} \ . \tag{14}$$

Correspondingly, we can write for the frequency-domain signal at the $l_{\text{th}}$ subcarrier

$$X^k_{\text{v,sum}}(l) = N_{\text{E}} A^k X^k_{\text{v}}(l) + N_{\text{E}} N^k_{\text{clip}}(l) \ , \tag{15}$$

where the DC component $N_{\text{E}} I_{\text{DC}}$ is not present for $l \in \mathcal{V}_{\text{info}}$ and $N^k_{\text{clip}}$ is the discrete Fourier transform of $n^k_{\text{c}}$. According to the central limit theorem (CLT), $N^k_{\text{clip}}$ can be modeled as an additive complex-valued Gaussian variable with zero mean and variance of $\sigma^2_{\text{clip},k}$ [43]. We now consider the two relaying schemes.

*a) DF Scheme:* In DF, the relay will only forward the message if it was detected correctly as verified by an outer error-detection code. Then, we will have $X^k_{\text{v}}(l) = \alpha X_{\text{p}}(m)$, where subcarrier $m \in \mathcal{P}_{\text{info}}$ from the PLC link is paired with subcarrier $l \in \mathcal{V}_{\text{info}}$ for the VLC link, and the factor $\alpha$ adjusts the VLC signal strength. The pairing will be discussed in more detail in Section IV. The received signal on subcarrier $l$ at user $u$ when served from luminaire $k$ follows as

$$\begin{aligned}Y^{k,u}_{\text{v}}(l) &= H^{k,u}_{\text{v}}(l) X^k_{\text{v,sum}}(l) + N^u_{\text{v}}(l) \\ &= N_{\text{E}}\alpha A^k H^{k,u}_{\text{v}}(l) X_{\text{p}}(m) + N_{\text{E}} H^{k,u}_{\text{v}}(l) N^k_{\text{clip}}(l) + N^u_{\text{v}}(l) \ ,\end{aligned} \tag{16}$$

where $H^{k,u}_{\text{v}}(l)$ is the VLC channel gain for subcarrier $l$ between the $k_{\text{th}}$ luminaire and user $u$, and $N^u_{\text{v}}(l)$ is the VLC noise on subcarrier $l$ at user $u$. The corresponding subcarrier SNR is

$$\text{SNR}^{k,u}_{\text{v}}(l) = \frac{|N_{\text{E}}\alpha A^k H^{k,u}_{\text{v}}(l)|^2 \sigma^2_{\text{p}}}{|N_{\text{E}} H^{k,u}_{\text{v}}(l)|^2 \sigma^2_{\text{clip},k} + \sigma^2_{\text{vn},u}} \ , \tag{17}$$

where $\sigma^2_{\text{vn},u} = \mathbb{E}\left[|N^u_{\text{v}}(l)|^2\right]$. As both clipping and VLC receiver noise can be approximated as i.i.d. Gaussian noise when $N_k \geq 64$ [45], the corresponding per-subcarrier rate can be calculated as (in bit per use)[1] [47]

$$\begin{aligned}&R^{k,u}(l,m) \\ =&\min\left(\log_2(1 + \text{SNR}^k_{\text{p}}(m)), \log_2(1 + \text{SNR}^{k,u}_{\text{v}}(l))\right) \ .\end{aligned} \tag{18}$$

.

*b) AF Scheme:* For AF, the relay always transmits $X^k_{\text{v}}(l) = \beta Y_{\text{p}}(m)$, where $\beta$ is the amplification factor for the AF scheme. Similar to (16), $Y^{k,u}_{\text{v}}(l)$ can be expressed as

$$\begin{aligned}Y^{k,u}_{\text{v}}(l) &= N_{\text{E}} A^k \beta H^{k,u}_{\text{v}}(l) H^k_{\text{p}}(m) X_{\text{p}}(m) \\ &+ N_{\text{E}} A^k \beta H^{k,u}_{\text{v}}(l) N^k_{\text{p}}(m) + N_{\text{E}} H^{k,u}_{\text{v}}(l) N^k_{\text{clip}}(l) + N^u_{\text{v}}(l) \ ,\end{aligned} \tag{19}$$

and the corresponding SNR at user $u$ is given by (20). Using again the fact that the total noise is Gaussian, the achievable rate follows as

$$R^{k,u}(l,m) = \log_2\left(1 + \text{SNR}^{k,u}_{\text{v}}(l,m)\right) \ . \tag{21}$$

*2) ACO-OFDM:* Different than DCO-OFDM, only odd subcarriers in ACO-OFDM carry information, i.e., $\mathcal{V}_{\text{info}} = \{1, 3, \ldots, 2N_{\text{v}} - 1\}$, which allows for zero-level clipping and reduces the minimum level of DC bias at the cost of reduced bandwidth efficiency [40]. The clipped ACO-OFDM signal can be expressed as [43]

$$x^k_{\text{v,clip}}(n) = 2A^k U(x^k_{\text{v,info}}(n)) x^k_{\text{v,info}}(n) + n^k_{\text{c}}(n) \ , \tag{22}$$

where $U(\cdot)$ is the Heaviside step function [48] and the variance of the clipping noise $n^k_{\text{c}}(n)$ is [43]

$$\begin{aligned}\sigma^2_{\text{clip},k} =& P^k_{\text{v}}\big(A^k\left((b^k)^2 + 1\right) - 2(A^k)^2 - b^k\left(\phi(b^k) - \phi(t^k)\right) \\ &- \phi(t^k)(t^k - b^k) + Q(t^k)(t^k - b^k)^2\big) \ .\end{aligned} \tag{23}$$

With this, the expression for the frequency-domain signal at the $l_{\text{th}}$ subcarrier for $l \in \mathcal{V}_{\text{info}}$ is the same as in (15). Accordingly, the SNR expressions for DF relaying in (17) and AF relaying in (20) also apply to ACO-OFDM and can be used in the rate expression (18) and (21), respectively, to obtain the associated achievable rate.

## IV. Subcarrier Allocation in HVP Systems

We now use the rate expressions from the previous section to optimize the rate of the overall HVP system. Since multiple users compete for resources, we integrate a notion of fairness into the rate optimization. In particular, we introduce a weight variable $w^u$ that represents the priority of user $u$. For example, in the case of a proportional fair (PF) scheduling policy that prioritizes the user with the lowest average data-rate, we have

[1]Both Eq. (18) and Eq. (21) can be derived from [47, Eq. (15)] and [47, Eq. (12)], respectively, via setting the direct link channel gain to 0. The absence of the coefficient $\frac{1}{2}$ is due to the full-duplex property of the luminaire relay.

$$\mathrm{SNR}_{\mathrm{v}}^{k,u}(l,m)=\frac{\left|N_{\mathrm{E}}A^{k}\beta H_{\mathrm{v}}^{k,u}(l)H_{\mathrm{p}}^{k}(m)\right|^{2}\sigma_{\mathrm{p}}^{2}}{\left|N_{\mathrm{E}}A^{k}\beta H_{\mathrm{v}}^{k,u}(l)\right|^{2}\sigma_{\mathrm{pn},k}^{2}(m)+\left|N_{\mathrm{E}}H_{\mathrm{v}}^{k,u}(l)\right|^{2}\sigma_{\mathrm{clip},k}^{2}+\sigma_{\mathrm{vn},u}^{2}}\,. \tag{20}$$

$w^u = 1/R^u_{\mathrm{avg}}(n)$ for long-term fairness consideration, where $R^u_{\mathrm{avg}}(n)$ is computed as

$$R^u_{\mathrm{avg}}(n)=\left(1-\frac{1}{N_{\mathrm{res}}}\right)R^u_{\mathrm{avg}}(n-1)+\frac{1}{N_{\mathrm{res}}}R^u(n-1)\,, \tag{24}$$

and $R^u(n)$ is the data rate at instance $n$ and $N_{\mathrm{res}}$ is the response time of the low-pass filter [49]. We note that the optimization framework presented in this section is independent of the specific scheduling policy that is applied.

The optimization of the achievable rate of the HVP system is accomplished through SA schemes, for which we propose two variants. The first variant, which we refer to as SA without SP, retains the subcarrier assignment when transitioning from PLC to VLC link. Assuming for simplicity and without loss of generality that $N_{\mathrm{v}} = N_{\mathrm{p}}$, we have $\mathcal{P}_{\text{info}} = \mathcal{V}_{\text{info}}$ and thus $l = m$ in (18) and (21) for DCO-OFDM. Since $\mathcal{V}_{\text{info}} = \{1, 3, \ldots, 2N_{\mathrm{v}} - 1\}$ for ACO-OFDM, we have $l = 2m - 1$, $m \in \mathcal{P}_{\text{info}}$, in this case. The second scheme applies subcarrier pairing at the relays, and we refer to it as SA with SP. It makes use of the fact that the per-subcarrier link qualities of the PLC and VLC hop are independent of each other.

Since the number of subcarriers in broadband HVP systems can be very large, an SA scheme considering each individual subcarrier will not only have large computational complexity, but also requires significant signaling overhead. To mitigate the computational and coordination complexity, a chunk-based SA scheme can be applied [20]. This means that a set of $N_{\mathrm{s}}$ adjacent subcarriers is grouped into a chunk, and the chunk is used as the minimum unit in SA. Hence, in the following we consider that $N_{\mathrm{c}}$ chunks are available in total, where $N_{\mathrm{p}} = N_{\mathrm{v}} = N_{\mathrm{s}}N_{\mathrm{c}}$, of which $C_k$ chunks are assigned to $k_{\mathrm{th}}$ luminaire, i.e., $N_k = N_{\mathrm{s}}C_k$. Obviously, $N_{\mathrm{s}} = 1$ is the special case of single-subcarrier-based allocation. Given that a codebook of size $S_c$ ($S_c = 2^q$) is employed for the channel gain vector space $\boldsymbol{H}^u_{\mathrm{v}}(l) = [H^{1,u}_{\mathrm{v}}(l), H^{2,u}_{\mathrm{v}}(l), \ldots, H^{N_{\mathrm{L}},u}_{\mathrm{v}}(l)]$, $qN_{\mathrm{c}}$ bits of CSI feedback are required for one OFDM block per VLC user. We define the binary variable $x^{k,u}_{i,j} \in \{0, 1\}$, $i, j \in \{1, 2, \ldots, N_{\mathrm{c}}\}$, with $x^{k,u}_{i,j} = 1$ indicating that $i_{\mathrm{th}}$ chunk in the PLC hop together with the $j_{\mathrm{th}}$ chunk in the VLC hop are assigned to user $u$ with the assistance of the $k_{\mathrm{th}}$ VLC-enabled luminaire. Furthermore, we will need in the following $\boldsymbol{x}_u = [x^{k,u}_{i,j}]_{i,j=1,\ldots,N_{\mathrm{c}},\, k=1,\ldots,N_{\mathrm{L}}}$ as the $N_{\mathrm{c}} \times N_{\mathrm{c}} \times N_{\mathrm{L}}$ SA tensor for user $u$ and $\boldsymbol{x} = [\boldsymbol{x}_1, \ldots, \boldsymbol{x}_{N_{\mathrm{U}}}]$ as the $N_{\mathrm{c}} \times N_{\mathrm{c}} \times N_{\mathrm{L}}N_{\mathrm{U}}$ tensor for SA across all users, and we will use the sets $\mathcal{N}_{\mathrm{c}} = \{1, 2, \ldots, N_{\mathrm{c}}\}$, $\mathcal{N}_{\mathrm{L}} = \{1, 2, \ldots, N_{\mathrm{L}}\}$ and $\mathcal{N}_{\mathrm{U}} = \{1, \ldots, N_{\mathrm{U}}\}$ in the following, where $\mathcal{N}_{\mathrm{c}}$, $\mathcal{N}_{\mathrm{L}}$ and $\mathcal{N}_{\mathrm{U}}$ are the sets of chunk indices, luminaire indices and user indices, respectively.

Next, we present the SA methods first for HVP with OFDM-TDMA and then for HVP with OFDMA.

### A. OFDM-TDMA

With OFDM-TDMA, the whole frequency spectrum is owned exclusively by the user with the highest priority weight $w^u$ in a certain time slot. Hence, SA is performed for one user only at a time.

*1) SA without SP:* For SA without SP, we have $x^{k,u}_{i,j} = 0$ for $i \neq j$, and the rate maximization problem can be formulated as

$$\begin{aligned}
&\mathrm{P1}: \boldsymbol{x}^*_u = \underset{\{\boldsymbol{x}_u\}}{\operatorname{argmax}} \sum_{i\in\mathcal{N}_{\mathrm{c}}}\sum_{k\in\mathcal{N}_{\mathrm{L}}} x^{k,u}_{i,i}R^{k,u}_{i,i} \qquad (25)\\
&\mathrm{C1}: \sum_{k\in\mathcal{N}_{\mathrm{L}}} x^{k,u}_{i,i} = 1, \forall i \in \mathcal{N}_{\mathrm{c}},\\
&\mathrm{C2}: \sum_{i\in\mathcal{N}_{\mathrm{c}}} x^{k,u}_{i,i} = C_k, \forall k \in \mathcal{N}_{\mathrm{L}},\\
&\mathrm{C3}: x^{k,u}_{i,i} \in \{0, 1\}, \forall i \in \mathcal{N}_{\mathrm{c}},\ \forall k \in \mathcal{N}_{\mathrm{L}}\,,
\end{aligned}$$

where $R^{k,u}_{i,j}$ represents the rate of the chunk pair $(i, j)$ for user $u$ and PLC-VLC relay $k$. Constraint C1 guarantees that each subcarrier pair is assigned to one and only one relay, and C2 ensures the number of subcarriers pairs allocated to each relay. P1 can be categorized as a linear semi-assignment problem and can be solved with a time complexity of $\mathcal{O}(N_{\mathrm{c}}^2 N_{\mathrm{L}})$ [50]. For the simulation results in the next section, we use the YALMIP [51] toolbox in conjunction with the MOSEK solver [52] to obtain a solution numerically.

*2) SA with SP:* Here we generalize P1 and allow subcarrier pairing at the relays. In this case, the optimization problem for user $u$ can be formulated as

$$\begin{aligned}
&\mathrm{P2}: \boldsymbol{x}^*_u = \underset{\{\boldsymbol{x}_u\}}{\operatorname{argmax}} \sum_{i\in\mathcal{N}_{\mathrm{c}}}\sum_{j\in\mathcal{N}_{\mathrm{c}}}\sum_{k\in\mathcal{N}_{\mathrm{L}}} x^{k,u}_{i,j}R^{k,u}_{i,j} \qquad (26)\\
&\mathrm{C1}: \sum_{j\in\mathcal{N}_{\mathrm{c}}}\sum_{k\in\mathcal{N}_{\mathrm{L}}} x^{k,u}_{i,j} = 1, \forall i \in \mathcal{N}_{\mathrm{c}}\,,\\
&\mathrm{C2}: \sum_{i\in\mathcal{N}_{\mathrm{c}}}\sum_{k\in\mathcal{N}_{\mathrm{L}}} x^{k,u}_{i,j} = 1, \forall j \in \mathcal{N}_{\mathrm{c}}\,,\\
&\mathrm{C3}: \sum_{i\in\mathcal{N}_{\mathrm{c}}}\sum_{j\in\mathcal{N}_{\mathrm{c}}} x^{k,u}_{i,j} = C_k, \forall k \in \mathcal{N}_{\mathrm{L}}\,,\\
&\mathrm{C4}: x^{k,u}_{i,j} \in \{0, 1\}, \forall i, j \in \mathcal{N}_{\mathrm{c}},\ \forall k \in \mathcal{N}_{\mathrm{L}}\,,
\end{aligned}$$

where C1 and C2 guarantee that each subcarrier is assigned to exactly one relay for the PLC and VLC hop, respectively, and C3 controls the number of assigned subcarrier pairs per relay. P2 can be categorized as a constrained linear 0-1 programming problem, which is NP-hard. We therefore apply a heuristic alternating optimization method to solve P2 suboptimally within polynomial time [53]. To this end, we introduce vectors $\{y^u_{i,j}\}$ and $\{z^{k,u}_i\}$ with $x^{k,u}_{i,j} = y^u_{i,j}z^{k,u}_i$, and P2 is transformed into

$$\text{P2.1}: (\boldsymbol{y}_u^*, \boldsymbol{z}_u^*) = \underset{\{\boldsymbol{y}_u, \boldsymbol{z}_u\}}{\operatorname{argmax}} \sum_{i\in\mathcal{N}_\mathrm{c}} \sum_{j\in\mathcal{N}_\mathrm{c}} \sum_{k\in\mathcal{N}_\mathrm{L}} y_{i,j}^u z_i^{k,u} R_{i,j}^{k,u}$$
$$\text{C1}: \sum_{j\in\mathcal{N}_\mathrm{c}} y_{i,j}^u = 1, \forall i \in \mathcal{N}_\mathrm{c},$$
$$\text{C2}: \sum_{i\in\mathcal{N}_\mathrm{c}} y_{i,j}^u = 1, \forall j \in \mathcal{N}_\mathrm{c},$$
$$\text{C3}: \sum_{k\in\mathcal{N}_\mathrm{L}} z_i^{k,u} = 1, \forall i \in \mathcal{N}_\mathrm{c},$$
$$\text{C4}: \sum_{i\in\mathcal{N}_\mathrm{c}} z_i^{k,u} = C_k, \forall k \in \mathcal{N}_\mathrm{L},$$
$$\text{C5}: y_{i,j}^u, z_i^{k,u} \in \{0,1\}, \forall i,j \in \mathcal{N}_\mathrm{c},\ \forall k \in \mathcal{N}_\mathrm{L}\ ,$$

where $\boldsymbol{y}_u = [y_{i,j}^u]_{i,j\in\mathcal{N}_\mathrm{c}}$ and $\boldsymbol{z}_u = [z_i^{k,u}]_{i\in\mathcal{N}_\mathrm{c},k\in\mathcal{N}_\mathrm{L}}$. P2.1 is a bilinear 0-1 programming problem, and we obtain a suboptimal solution by alternately optimizing on $\boldsymbol{y}_u$ and $\boldsymbol{z}_u$. When $\boldsymbol{y}_u$ is fixed, we can ignore constraints C1 and C2, and P2.1 will degenerate to P1 with $R_{i,i}^{k,u}$ replaced by $T_i^{k,u} = \sum_{j\in\mathcal{N}_\mathrm{c}} y_{i,j}^u R_{i,j}^{k,u}$, which will be referred to as P2.2. When $\boldsymbol{z}_u$ is fixed, we define $S_{i,j}^u = \sum_{k\in\mathcal{N}_\mathrm{L}} z_i^{k,u} R_{i,j}^{k,u}$ and P2.1 becomes

$$\text{P2.3}: \boldsymbol{y}_u^* = \underset{\{\boldsymbol{y}_u\}}{\operatorname{argmax}} \sum_{i\in\mathcal{N}_\mathrm{c}} \sum_{j\in\mathcal{N}_\mathrm{c}} y_{i,j}^u S_{i,j}^u$$
$$\text{C1}: \sum_{j\in\mathcal{N}_\mathrm{c}} y_{i,j}^u = 1, \forall i \in \mathcal{N}_\mathrm{c},$$
$$\text{C2}: \sum_{i\in\mathcal{N}_\mathrm{c}} y_{i,j}^u = 1, \forall j \in \mathcal{N}_\mathrm{c},$$
$$\text{C3}: y_{i,j}^u \in \{0,1\}, \forall i,j \in \mathcal{N}_\mathrm{c}\ ,$$

which is a classic assignment problem and can be solved by the Hungarian algorithm with a computational complexity of $\mathcal{O}(N_\mathrm{c}^3)$ [54], [55]. The algorithm of the alternating optimization for P2 is summarized in Algorithm 1 and the time complexity is $\mathcal{O}(N_\mathrm{c}^3 + N_\mathrm{c}^2 N_\mathrm{L})$.

**Algorithm 1** Alternating Optimization for P2

1. **Initialization**:
   $u^* = \operatorname{argmax}_{u\in\mathcal{N}_\mathrm{U}}\{w^u\}$.
   Calculate $\{R_{i,j}^{k,u^*}\}$.
   $\boldsymbol{y}_{u^*}^0 \Leftarrow \boldsymbol{I}_{N_\mathrm{c}\times N_\mathrm{c}}$, $p \Leftarrow 0$.
2. **repeat**
3. Update $\{T_i^{k,u^*}\}$ with $\boldsymbol{y}_{u^*}^p$.
4. Solve P2.2 according to [50] and get $\boldsymbol{z}_{u^*}^p$.
5. Update $\{S_{i,j}^{u^*}\}$ with $\boldsymbol{z}_{u^*}^p$.
6. Solve P2.3 and get $\boldsymbol{y}_{u^*}^{p+1}$.
7. $p \Leftarrow p+1$.
8. **until** $\|\boldsymbol{y}_{u^*}^{p+1} - \boldsymbol{y}_{u^*}^p\| \le \delta$ ($\delta$ is a predefined threshold)
9. Compute $\boldsymbol{x}_{u^*}$ according to $x_{i,j}^{k,u^*} = y_{i,j}^{u^*} z_i^{k,u^*}$.
10. Update $\{w^u\}_{u\in\mathcal{N}_\mathrm{U}}$ according to rate update (24).

### B. OFDMA

OFDMA accomplishes multiple access by assigning different subcarriers to different users. This allows for a more flexible SA scheme that can exploit multi-user diversity.

*1) SA without SP:* Without SP at the relays, again $x_{i,j}^{k,u} = 0$ for $i \neq j$, and the maximization problem for the weighted sum rate is

$$\text{P3}: \boldsymbol{x}^* = \underset{\{\boldsymbol{x}\}}{\operatorname{argmax}} \sum_{u\in\mathcal{N}_\mathrm{U}} w^u \sum_{i\in\mathcal{N}_\mathrm{c}} \sum_{k\in\mathcal{N}_\mathrm{L}} x_{i,i}^{k,u} R_{i,i}^{k,u} \quad (27)$$
$$\text{C1}: \sum_{u\in\mathcal{N}_\mathrm{U}} \sum_{k\in\mathcal{N}_\mathrm{L}} x_{i,i}^{k,u} = 1, \forall i \in \mathcal{N}_\mathrm{c},$$
$$\text{C2}: \sum_{u\in\mathcal{N}_\mathrm{U}} \sum_{i\in\mathcal{N}_\mathrm{c}} x_{i,i}^{k,u} = C_k, \forall k \in \mathcal{N}_\mathrm{L}\ ,$$
$$\text{C3}: x_{i,i}^{k,u} \in \{0,1\}, \forall i \in \mathcal{N}_\mathrm{c},\ k \in \mathcal{N}_\mathrm{L},\ u \in \mathcal{N}_\mathrm{U}\ ,$$

Similar to problem P2, we introduce vectors $\{a_{i,u}\}$ and $\{b_{i,k}\}$ with $x_{i,i}^{k,u} = a_{i,u} b_{i,k}$, and suboptimally solve P3 with alternating optimization based on the transformation into

$$\text{P3.1}: (\boldsymbol{a}^*, \boldsymbol{b}^*) = \underset{\{\boldsymbol{a},\boldsymbol{b}\}}{\operatorname{argmax}} \sum_{u\in\mathcal{N}_\mathrm{U}} w^u \sum_{i\in\mathcal{N}_\mathrm{c}} \sum_{k\in\mathcal{N}_\mathrm{L}} a_{i,u} b_{i,k} R_{i,i}^{k,u}$$
$$\text{C1}: \sum_{u\in\mathcal{N}_\mathrm{U}} a_{i,u} = 1, \forall i \in \mathcal{N}_\mathrm{c}\ ,$$
$$\text{C2}: \sum_{k\in\mathcal{N}_\mathrm{L}} b_{i,k} = 1, \forall i \in \mathcal{N}_\mathrm{c}\ ,$$
$$\text{C3}: \sum_{i\in\mathcal{N}_\mathrm{c}} b_{i,k} = C_k, \forall k \in \mathcal{N}_\mathrm{L}\ ,$$
$$\text{C4}: a_{i,u}, b_{i,k} \in \{0,1\}, \forall i \in \mathcal{N}_\mathrm{c},\ k \in \mathcal{N}_\mathrm{L},\ u \in \mathcal{N}_\mathrm{U}\ .$$

where $\boldsymbol{a} = [a_{i,u}]_{i\in N_\mathrm{c}, u\in N_\mathrm{U}}$ and $\boldsymbol{b} = [b_{i,k}]_{i\in N_\mathrm{c}, k\in N_\mathrm{L}}$. Let $E_i^u = \sum_{k\in\mathcal{N}_\mathrm{L}} b_{i,k} R_{i,i}^{k,u}$, $F_i^k = \sum_{u\in\mathcal{N}_\mathrm{U}} a_{i,u} w^u R_{i,i}^{k,u}$, and function $u_i^* = \operatorname{argmax}_{u\in\mathcal{N}_\mathrm{U}}\{w^u E_i^u\}$. We observe that the optimal solution of P3.1 with $\boldsymbol{b}$ fixed is a vector $\boldsymbol{a}^*$ with $a_{i,u_i^*} = 1$ and zero otherwise. When $\boldsymbol{a}$ is fixed, we can ignore constraints C1 in P3.1, and P3.1 will degenerate to P1 with $R_{i,i}^{k,u}$ replaced by $F_i^k$ and $x_{i,i}^{k,u}$ replaced by $b_{i,k}$, which will be referred to as P3.2. The algorithm of the alternating optimization for P3 is summarized in Algorithm 2, and the time complexity is $\mathcal{O}(N_\mathrm{c}^2 N_\mathrm{L} + N_\mathrm{c} N_\mathrm{U} N_\mathrm{L})$.

**Algorithm 2** Alternating Optimization for P3

1. **Initialization**:
   Calculate $\{R_{i,i}^{k,u}\}$.
   $\boldsymbol{a}^0 \Leftarrow \boldsymbol{I}_{N_\mathrm{c}\times N_\mathrm{U}}$, $p \Leftarrow 0$.
2. **repeat**
3. Update $\{F_i^k\}$ with $\boldsymbol{a}^p$.
4. Solve P3.2 according to [50] and get $\boldsymbol{b}^p$.
5. Update $\{E_i^u\}$ with $\boldsymbol{b}^p$.
6. Find $u_i^*$ and obtain $\boldsymbol{a}^{p+1}$.
7. $p \Leftarrow p+1$.
8. **until** $\|\boldsymbol{a}^{p+1} - \boldsymbol{a}^p\| \le \delta$ ($\delta$ is a predefined threshold)
9. Compute $\boldsymbol{x}$ according to $x_{i,i}^{k,u} = a_{i,u} b_{i,k}$.
10. Update $\{w^u\}_{u\in\mathcal{N}_\mathrm{U}}$ according to rate update in (24).

*2) SA with SP:* Allowing subcarrier pairing at the relays, the weighted sum rate maximization problem can be expressed as

$$\text{P4}: \boldsymbol{x}^* = \underset{\{\boldsymbol{x}\}}{\text{argmax}} \sum_{u\in\mathcal{N}_\text{U}} w^u \sum_{i\in\mathcal{N}_\text{c}} \sum_{j\in\mathcal{N}_\text{c}} \sum_{k\in\mathcal{N}_\text{L}} x_{i,j}^{k,u} R_{i,j}^{k,u}$$

$$\text{C1}: \sum_{u\in\mathcal{N}_\text{U}} \sum_{j\in\mathcal{N}_\text{c}} \sum_{k\in\mathcal{N}_\text{L}} x_{i,j}^{k,u} = 1, \forall i \in \mathcal{N}_\text{c} \ ,$$

$$\text{C2}: \sum_{u\in\mathcal{N}_\text{U}} \sum_{i\in\mathcal{N}_\text{c}} \sum_{k\in\mathcal{N}_\text{L}} x_{i,j}^{k,u} = 1, \forall j \in \mathcal{N}_\text{c} \ ,$$

$$\text{C3}: \sum_{u\in\mathcal{N}_\text{U}} \sum_{i\in\mathcal{N}_\text{c}} \sum_{j\in\mathcal{N}_\text{c}} x_{i,j}^{k,u} = C_k, \forall k \in \mathcal{N}_\text{L} \ ,$$

$$\text{C4}: x_{i,j}^{k,u} \in \{0,1\}, \forall i,j \in \mathcal{N}_\text{c},\ k \in \mathcal{N}_\text{L},\ u \in \mathcal{N}_\text{U} \ .$$

P4 is a constrained linear 0-1 programming problem, which is NP-hard. Here we propose a heuristic subcarrier offloading algorithm that can solve the problem suboptimally within polynomial time. First we relax the constraints of P4 and consider P4 without C3, which will be referred to as P4.1. P4.1 can be solved with the algorithm proposed in [56] within a polynomial time of $\mathcal{O}(N_\text{L}N_\text{U}N_\text{c}^2+N_\text{c}^3)$, and the solution is denoted as $\{\tilde{x}_{i,j}^{k,u}\}$. Define $\mathcal{N}_{\text{L}1}$ and $\mathcal{N}_{\text{L}2}$ as the sets of luminaires that do and do not exceed the assigned value $C_k$, respectively, with $\mathcal{N}_{\text{L}1} = \{k|c_k > C_k\}$, $\mathcal{N}_{\text{L}2} = \{k|c_k < C_k\}$, where $c_k = \sum_{u\in\mathcal{N}_\text{U}} \sum_{i\in\mathcal{N}_\text{c}} \sum_{j\in\mathcal{N}_\text{c}} \tilde{x}_{i,j}^{k,u}$. Define $\hat{R}_{i,j}^{k,u} = w^u \tilde{R}_{i,j}^{k,u}$ and set $\mathcal{R} = \{\hat{R}_{i,j}^{k,u} | \tilde{x}_{i,j}^{k,u} = 1, k \in \mathcal{N}_{\text{L}1}\}$. Then we can execute the subcarrier offloading algorithm summarized in Algorithm 3 and obtain the solution $\boldsymbol{x}^*$ to P4. The time complexity of Algorithm 3 is $\mathcal{O}(N_\text{c}N_\text{L}N_\text{U} + N_\text{c}\log(N_\text{c}))$. So the total time complexity of solving P4 will be $\mathcal{O}(N_\text{L}N_\text{U}N_\text{c}^2 + N_\text{c}^3)$.

**Algorithm 3** Subcarrier Offloading Algorithm

1. Sort $\mathcal{R}$ in increasing order and store it in array $\mathcal{A}_R$
2. **for** $\hat{R}_{i,j}^{k,u}$ **in** $\mathcal{A}_R$
3. Initialize $\hat{R}_{i,j}^{\max} \Leftarrow 0$, $(k^*, u^*) \Leftarrow (0,0)$
4. **for** $k' \in \mathcal{N}_{\text{L}2}$, $u' \in N_\text{U}$
5. **if** $\hat{R}_{i,j}^{k',u'} > \hat{R}_{i,j}^{\max}$
6. $\hat{R}_{i,j}^{\max} \Leftarrow \hat{R}_{i,j}^{k',u'}$, $(k^*, u^*) \Leftarrow (k', u')$
7. **end if**
8. **end for**
9. $\tilde{x}_{i,j}^{k,u} \Leftarrow 0$, $\tilde{x}_{i,j}^{k^*,u^*} \Leftarrow 1$, update $c_k$, $\mathcal{N}_{\text{L}1}$ and $\mathcal{N}_{\text{L}2}$.
10. **if** $\mathcal{N}_{\text{L}1} = \emptyset$
11. **break**
12. **end if**
13. **end for**
14. update $\{x_{i,j}^{k,u}\} \Leftarrow \{\tilde{x}_{i,j}^{k,u}\}$.

## V. Numerical Results and Discussions

We now evaluate the performance of the proposed SO-OFDM-based HVP system. We consider an example setup of a 5 m × 5 m room with $N_\text{L} = 4$ coordinated VLC-enabled LED luminaires, each of which contains $N_\text{E} = 36$ LEDs. The

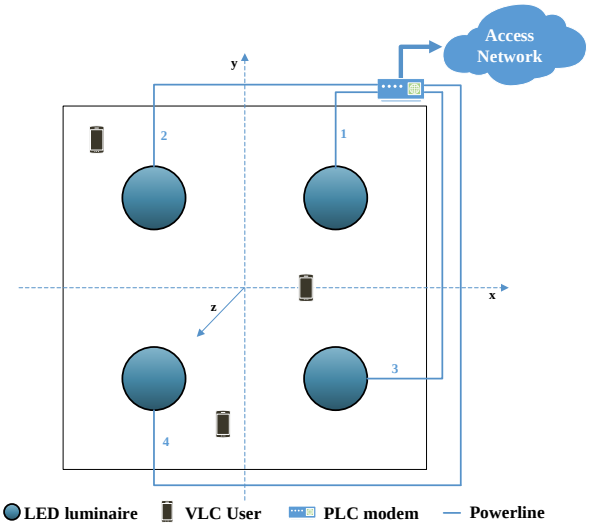


Fig. 3. The setup of HVP system.

setup of the HVP system and the applied coordinate system are illustrated in Fig. 3. Denoting the length of the power line connecting the $i_\text{th}$ luminaire and the PLC modem as $l_i$, we consider an example setup where $l_1 = 7$ m, $l_2 = 8$ m, $l_3 = 9$ m, $l_4 = 10$ m. The LEDs have an operating range of $I_\text{L} = 300$ mA to $I_\text{U} = 700$ mA, with a 3 dB bandwidth $\text{W}_\text{LED} = 10$ MHz with blue filtering [57]. The DC bias is set to $I_\text{DC} = (I_\text{L} + I_\text{U})/2 = 500$ mA, which provides a sufficient illumination for office work and study with this system setup [5].

The HVP system has $N_\text{p} = 1024$ independent information-carrying subcarriers, and we set $C_k = 256$, $k = 1, \ldots, 4$. For the PLC link, the minimum subcarrier frequency is 2.026 MHz and the subcarrier spacing is 24.4 kHz [30]. For the VLC link, we adopt the same subcarrier spacing as the PLC link, but the first data carrying subcarrier is at frequency 24.4 kHz. The PLC transmit PSD is set to -50 dBm/Hz according to the HomePlug AV standard [58] so that conducted and radiated emission limits are met. The PLC noise in the simulation includes background, narrowband, and impulse noise, where the PSDs and the corresponding measurement-based parameters of the former two are described in [59] and [29], respectively. For the impulse noise, we adopt the model from the IEEE 1901 standard [30, Annex F.3.5.2], which includes periodic synchronous, periodic asynchronous and aperiodic noise components, and we apply the parameters from measurements provided in [60]. The PLC noise simulator we developed and used here is available online [33]. For simulation accuracy, we apply the two-state approximation as in [32, Eq. (19)] to calculate the average achievable rate, which takes into account all of colored background noise, narrowband disturbance and impulsive noise. The average achievable rate can be calculated as the weighted sum of the achievable rates of the system with and without impulse noise:

$$R_\text{avg} = (1-p)R_\text{without\_imp} + pR_\text{with\_imp} \ , \tag{28}$$

where $R_\text{avg}$ denotes the average achievable rate, $R_\text{without\_imp}$

denotes the achievable rate of the system when impulse noise is absent and only colored background noise and narrowband disturbance are considered, and $R_{\text{with\_imp}}$ denotes the achievable rate of the system when impulse noise is present. $p$ denotes the probability of impulse noise occurrence, and we let $p = 0.01$ in the simulation based on the PLC noise measurement [31]. According to the measurement, $p < 0.01$ in even heavily disturbed power line environment, thus our simulation results can be considered as a lower bound of the average achievable rate. Further system parameters are listed in Table I.

TABLE I
SIMULATION PARAMETERS.

| Room Setup | |
|---|---|
| Fixture coordinate 1 | [1.25, 1.25, 3] |
| Fixture coordinate 2 | [1.25, -1.25, 3] |
| Fixture coordinate 3 | [-1.25, -1.25, 3] |
| Fixture coordinate 4 | [-1.25, 1.25, 3] |
| Room Length L × W × H | 5 [m] × 5 [m] × 3 [m] |

| VLC Parameters | |
|---|---|
| Lambertian order $m$ | 1 |
| PD area $A_{\text{PD}}$ | 1 [cm$^2$] |
| Concentrator refractive index $\kappa$ | 1.5 |
| Receiver FOV $\psi_c$ | 85 [deg.] |
| Noise bandwidth factor $I_2$ | 0.562 |
| Background current $I_{\text{bg}}$ | 100 [$\mu$A] |
| LED conversion factor $s$ | 0.44 [W/A] |
| PD responsivity $\gamma$ | 0.30 [A/W] |

### A. Single-User System

We first consider the single-user scenario and focus on analyzing the system performance with different optical OFDM, relay and SA schemes. In the following, we use *DF-DCO*, *DF-ACO*, *AF-DCO* and *AF-ACO* to identify the cases where DF or AF relaying at the luminaires is used together with DCO-OFDM or ACO-OFDM for the optical OFDM scheme, respectively.

Fig. 4 compares the achievable rates of the four transmission schemes as a function of the user location in the x-y plane. The user height is assumed to be $z = 0.8$ m. We observe that for all four schemes, the system achieves the highest rate when the user is near the center of the room and rate decreases as the user moves closer to the walls. *SA without SP* and *SA with SP* can improve the achievable rate notably across the room compared with a random SA at the luminaire relays, which we refer to as *Random SA*. In Fig. 4, we also notice that the DCO-OFDM scheme achieves a higher system rate than ACO-OFDM. This is due to the fact that ACO-OFDM only utilizes odd subcarriers for data transmission, which makes it less bandwidth-efficient than DCO-OFDM. In particular, for the same number of information-carrying subcarriers in DCO-OFDM and ACO-OFDM, ACO-OFDM uses a broader frequency spectrum and thus suffers from stronger channel attenuation at higher frequencies. For the results in Fig. 4, we

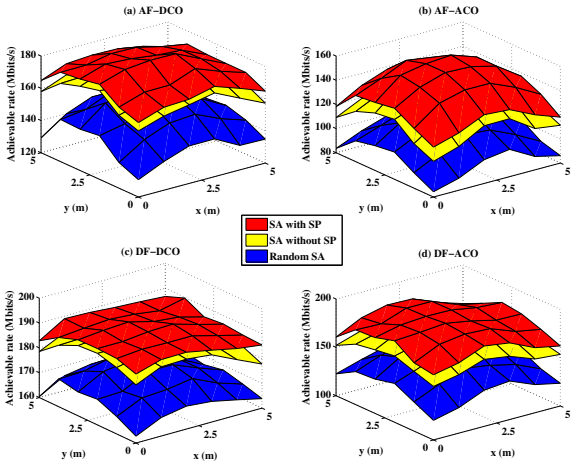


Fig. 4. Achievable rate as a function of user location. $N_{\text{c}} = 16$, $\alpha = \sqrt{10}$, $\beta = 10$.

set $\alpha = \sqrt{10}$ and $\beta = 10$, which is a reasonable choice as will be discussed next.

For the results in Fig. 5 and Fig. 6, we fix the user location to $x = -0.5$ m, $y = 1.5$ m, and $z = 0.8$ m. In Fig. 5, we show the achievable rate as a function of the relay gain $\alpha$ and $\beta$, respectively. When the relay gain is small and thus the transmission power for the VLC hop is relatively low, the system performance is VLC-noise limited. Increasing the relay gain will increase the SNR, but at some point the LED clipping distortion becomes the dominant noise source and curbs further performance improvements. Hence, there is an optimal relay gain for each of the four transmissions schemes, which depends on magnitude of VLC noise, VLC channel (e.g., receiver orientation, etc). Fig. 6 compares the performance of *Random SA*, *SA without SP* and *SA with SP* as a function of chunk size $N_{\text{s}}$. We can observe that *SA without SP* and *SA with SP* can greatly enhance the system performance compared with *Random SA*. Note that for *SA without SP* in the AF-DCO system, modulation/demodulation, FFT/IFFT and encode/decode blocks shown in Fig. 2 are not required, and the signal transition between PLC and VLC can be done in the analogue domain. Based on the results, a chunk size of $N_{\text{s}} = 16$ seems to provide close to optimal performance, while providing computational complexity savings when solving the SA optimization problem.

We next investigate whether the PLC or the VLC hop is limiting the performance of the HVP system, for which we focus on the DF-mode and SA with SP. Since the PLC and VLC channels are frequency selective, we count the number $N_{\text{VLC\_BL}}$ of subcarrier pairs for which the VLC hop is the bottleneck link when the maximum achievable rate is attained. Fig. 7 plots the $N_{\text{VLC\_BL}}$ as a function of the user location in the x-y plane with $z = 0.8$ m for both DF-DCO and DF-ACO. The 3 dB bandwidth of $\text{W}_{\text{LED}} = 10$ MHz used for the results in Fig. 7a corresponds to the current system setup with a blue filter at the photodiode, and $\text{W}_{\text{LED}} = 2$ MHz for the results in Fig. 7b corresponds to a photodiode receiver without

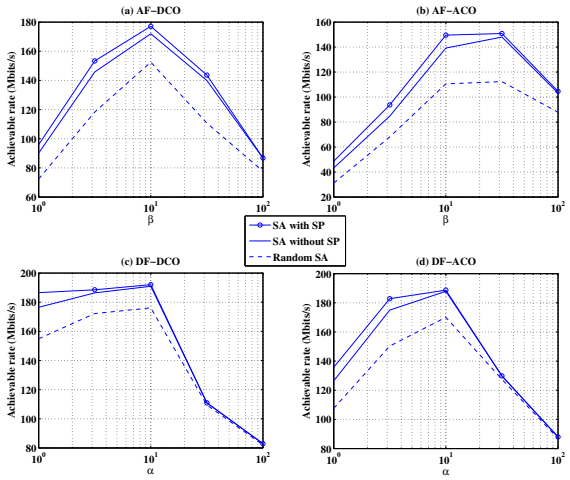


Fig. 5. Achievable rate versus relay gain ($\alpha$ or $\beta$). $N_{\mathrm{c}} = 16$. User location is $x = -0.5$ m, $y = 1.5$ m, $z = 0.8$ m.

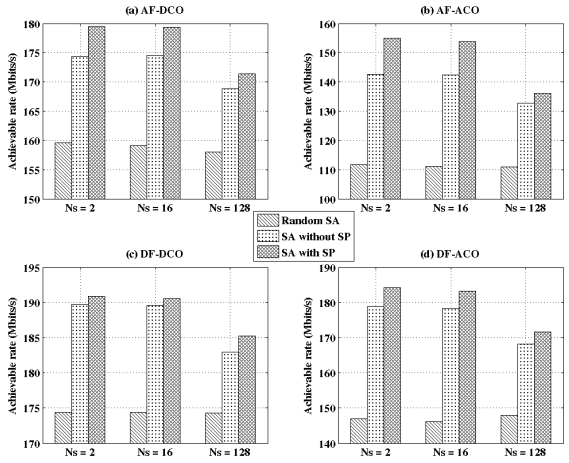


Fig. 6. Comparison of different SA schemes with different chunk size $N_{\mathrm{s}}$. $\alpha = \sqrt{10}$, $\beta = 10$. User location is $x = -0.5$ m, $y = 1.5$ m, $z = 0.8$ m.

blue filtering [61]. We observe that $N_{\mathrm{VLC\_BL}}$ of DF-DCO is generally smaller than that of DF-ACO due to the stronger channel attenuation of ACO-OFDM at higher frequencies. In Fig. 7a, $N_{\mathrm{VLC\_BL}}$ is typically less than 60 out of $N_{\mathrm{p}} = 1024$ subcarrier pairs for both DF-DCO and DF-ACO, which shows that the PLC link is the main bottleneck for the end-to-end performance of the HVP system. This changes notably and especially for the system operating in the DF-ACO mode when the LED bandwidth is reduced to 2 MHz. Here, the VLC hop limits the system performance, as shown in Fig. 7b.

### B. Multi-User System

We now consider the scenario of multiple VLC users. We perform simulations for both OFDM-TDMA and OFDMA to evaluate the corresponding achievable rate and user fairness. In this section, we use *AF-ACO* as the example transmission scheme. Fig. 8 shows the average sum achievable rate against

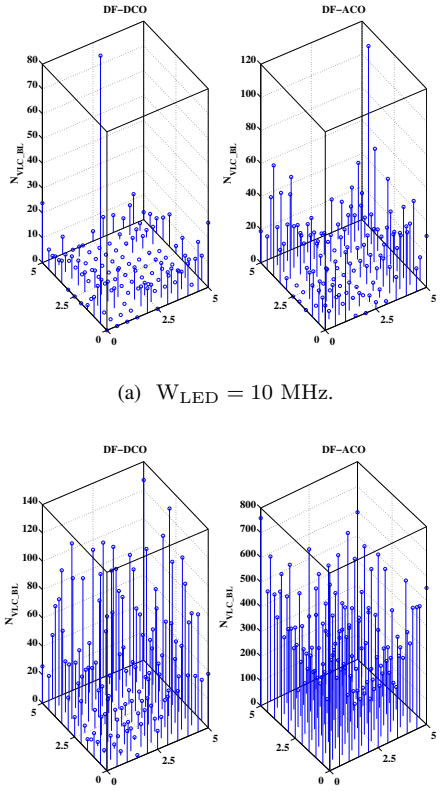


(a) $\mathrm{W_{LED}} = 10$ MHz.

(b) $\mathrm{W_{LED}} = 2$ MHz.

Fig. 7. $N_{\mathrm{VLC\_BL}}$ as a function of user location. $N_{\mathrm{c}} = 16$. $N_{\mathrm{VLC\_BL}}$ is the number of subcarrier pairs for which the VLC hop is the bottleneck link when the maximum achievable rate is attained.

the number of VLC users. For a given value of $N_{\mathrm{U}}$, a set of sum achievable rates are calculated and averaged by distributing $N_{\mathrm{U}}$ users uniformly at random over the indoor environment. For a fixed location of $N_{\mathrm{U}}$ users, we evaluate the average sum achievable rate over 100 time slots, and the weights $\{w^u\}$ in schemes with PF scheduling are updated with $N_{\mathrm{res}} = 20$ in (24). For schemes without PF, *OFDM-TDMA without PF* represents an OFDM-TDMA scheme with $w^u$ set to 1 and the user scheduling degrades to a Round-Robin (RR) scheme. *OFDMA without PF* represents an OFDMA scheme with $w^u$ set to 1, and the user scheduling degrades to a sum-rate maximizing scheduling and fairness across users is neglected. From Fig. 8, we can see that as $N_{\mathrm{U}}$ increases, the sum achievable rates of OFDMA schemes grow monotonically while the sum achievable rates of OFDM-TDMA remain almost unchanged. OFDMA outperforms OFDM-TDMA since it exploits the multi-user diversity. Not imposing the PF constraint provides further gains due to the increased multi-user diversity.

The benefit of schemes with PF is illustrated in Fig. 9. We consider a fixed location profile for $N_{\mathrm{U}} = 4$ users and plot the average achievable rate for each user over 100 time slots (we assume that users remain static during this time period). We can see that PF can improve the data rate fairness across users for both OFDM-TDMA and OFDMA schemes, and PF is significantly important for OFDMA scheme. For the setup in Fig. 9, due to the poor channel conditions, no

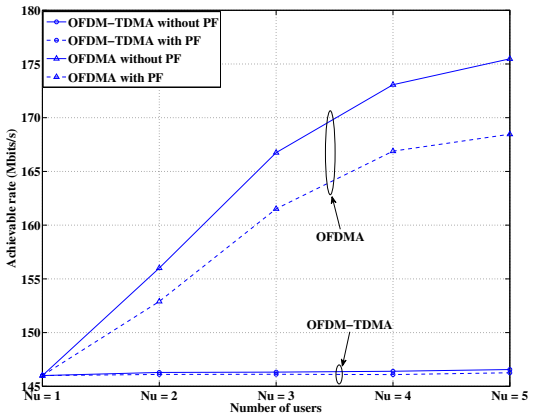


Fig. 8. Achievable rate versus the number of users $N_{\mathrm{U}}$. *SA with SP* and *AF-ACO* are applied. $\beta = 10$, $N_{\mathrm{c}} = 16$.

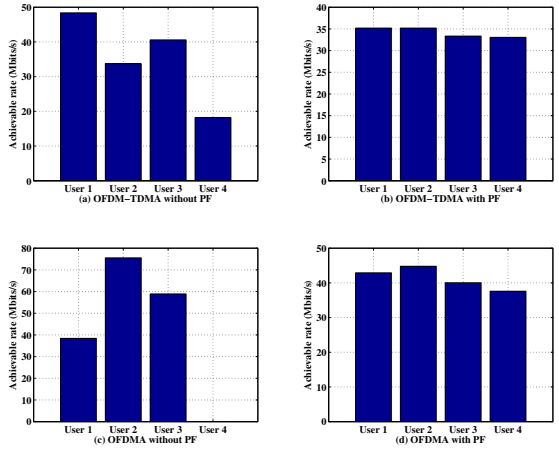


Fig. 9. Comparison of multi-access schemes with and without PF for $N_{\mathrm{U}} = 4$. The example locations are $(x = -1.25, y = 1.25, z = 0.8)$ m, $(x = -1.25, y = -1.25, z = 0.8)$ m, $(x = 1.25, y = 1.25, z = 0.8)$ m and $(x = 2.5, y = 2.5, z = 0.8)$ m for User 1, User 2, User 3 and User 4, respectively. *SA with SP* and *AF-ACO* are applied. $N_{\mathrm{c}} = 16$, $\beta = 10$.

subcarrier is allocated to User 4 in the OFDMA scheme without PF. Unlike RF wireless communication, there is no multipath fading for indoor VLC channels due to the large photodiode size compared with the optical wavelength. The deterministic nature of the VLC channel will fix users in low SNR channels to become complete neglected in user scheduling if PF scheduling is not applied. As expected, although PF results in lower overall rate, it is a desirable feature to ensure some level of fairness among the users of the proposed HVP system.

## VI. Conclusion

In this paper, we have proposed a multicarrier HVP system as a potential indoor high-speed downlink solution employing the symbiotic relationship between PLC and VLC. Compared with traditional multicarrier-based VLC-PLC integration, the proposed HVP system alleviates the PAPR problem for VLC transmitters and eliminates the inter-luminaire interference through the cooperation of LED luminaires piggybacked on the powerline backbone. We have considered the HVP system as a two-hop relay system and investigated different approaches of signal transition between PLC and VLC systems. To exploit the frequency selectivity of HVP channels, as well as the multi-user and multi-transmitter diversity, we have proposed several subcarrier allocation schemes with varying degrees of tradeoff among hardware, computational complexity and performance for meaningful variations of the HVP system. As another important contribution, we have investigated and compared two multi-access schemes for the HVP system, i.e., OFDMA and OFDM-TDMA. Several polynomial-time SA algorithms are proposed correspondingly. At the cost of higher computational complexity, OFDMA has been shown to outperform OFDM-TDMA for the HVP system in multi-user situations. For future work, power and bit loading for the SO-OFDM-based HVP system can be investigated, where the linear periodically time varying (LPTV) properties of PLC channels can be exploited to reduce the complexity of implementation [62].

## References

[1] H. Ma, L. Lampe, and S. Hranilovic, "Subcarrier allocation in hybrid visible light and power line communication system," in *IEEE International Symposium on Circuits and Systems (ISCAS), Montreal, Canada*, accepted 2016.

[2] M. Rahaim, A. M. Vegni, and T. Little, "A hybrid radio frequency and broadcast visible light communication system," in *IEEE GLOBECOM Workshops*, Dec. 2011, pp. 792–796.

[3] X. Li, R. Zhang, and L. Hanzo, "Cooperative load balancing in hybrid visible light communications and WiFi," *IEEE Trans. Commun.*, vol. 63, no. 4, pp. 1319–1329, Apr. 2015.

[4] D. A. Basnayaka and H. Haas, "Design and analysis of a hybrid radio frequency and visible light communication system," *IEEE Trans. Commun.*, vol. PP, no. 99, pp. 1–1, 2017.

[5] H. Ma, L. Lampe, and S. Hranilovic, "Coordinated broadcasting for multiuser indoor visible light communication systems," *IEEE Trans. Commun.*, vol. 63, no. 9, pp. 3313–3324, Sept 2015.

[6] Z. Yu, R. J. Baxley, and G. T. Zhou, "Multi-user MISO broadcasting for indoor visible light communication," in *IEEE International Conference on Acoustics, Speech and Signal Processing (ICASSP)*, May 2013.

[7] H. Ma, L. Lampe, and S. Hranilovic, "Robust MMSE linear precoding for visible light communication broadcasting systems," in *IEEE Global Communications Conference (Globecom)*, Atlanta, GA, USA, Dec. 2013.

[8] M. Kashef, M. Abdallah, K. Qaraqe, H. Haas, and M. Uysal, "Coordinated interference management for visible light communication systems," *IEEE J. Opt. Commun. Netw.*, vol. 7, no. 11, pp. 1098–1108, 2015.

[9] W. Ding, F. Yang, H. Yang, J. Wang, X. Wang, X. Zhang, and J. Song, "A hybrid power line and visible light communication system for indoor hospital applications," *Computers in Industry*, vol. 68, pp. 170–178, 2015.

[10] A. Familua, A. Ndjiongue, K. Ogunyanda, L. Cheng, H. Ferreira, and T. Swart, "A semi-hidden markov modeling of a low complexity FSK-OOK in-house PLC and VLC integration," in *IEEE International Symposium on Power Line Communications and Its Applications (ISPLC)*, 2015, pp. 199–204.

[11] L. Yonge, J. Abad, K. Afkhamie, L. Guerrieri, S. Katar, H. Lioe, P. Pagani, R. Riva, D. M. Schneider, and A. Schwager, "An overview of the homeplug av2 technology," *Journal of Electrical and Computer Engineering*, 2013.

[12] C. Cano, A. Pittolo, D. Malone, L. Lampe, A. M. Tonello, and A. G. Dabak, "State of the art in power line communications: From the applications to the medium," *IEEE J. Sel. Areas Commun.*, vol. 34, no. 7, pp. 1935–1952, 2016.

[13] T. Komine and M. Nakagawa, "Integrated system of white LED visible-light communication and power-line communication," *IEEE Trans. Consum. Electron.*, vol. 49, no. 1, pp. 71–79, 2003.

[14] P. Amirshahi and M. Kavehrad, "Broadband access over medium and low voltage power-lines and use of white light emitting diodes for indoor communications," in *Proc. 3rd IEEE Consumer Communications and Networking Conference*, vol. 2, 2006, pp. 897–901.

[15] H. Ma, L. Lampe, and S. Hranilovic, "Integration of indoor visible light and power line communication systems," in *17th IEEE International Symposium on Power Line Communications and Its Applications (ISPLC)*, 2013, pp. 291–296.

[16] H. Ferreira, L. Lampe, J. Newbury, and T. Swart, *Power Line Communications: Theory and Applications for Narrowband and Broadband Communications over Power Lines*. John Wiley & Sons, 2011.

[17] H. Elgala, R. Mesleh, and H. Haas, "Indoor broadcasting via white LEDs and OFDM," *IEEE Trans. Consum. Electron.*, vol. 55, no. 3, pp. 1127–1134, 2009.

[18] D. Tsonev, H. Chun, S. Rajbhandari, J. J. McKendry, S. Videv, E. Gu, M. Haji, S. Watson, A. E. Kelly, G. Faulkner *et al.*, "A 3-Gb/s single-LED OFDM-based wireless VLC link using a gallium nitride," *IEEE Photon. Technol. Lett.*, vol. 26, no. 7, pp. 637–640, 2014.

[19] M. Mossaad, S. Hranilovic, and L. Lampe, "Visible light communications using OFDM and multiple LEDs," *IEEE Trans. Commun.*, vol. 63, no. 11, pp. 4304–4313, Nov 2015.

[20] M. Herdin, "A chunk based OFDM amplify-and-forward relaying scheme for 4G mobile radio systems," in *International Conference on Communications*, vol. 10, 2006, pp. 4507–4512.

[21] T. Komine and M. Nakagawa, "Fundamental analysis for visible-light communication system using LED lights," *IEEE Trans. Consum. Electron.*, vol. 50, no. 1, pp. 100–107, 2004.

[22] P. Marsch and G. P. Fettweis, *Coordinated Multi-Point in Mobile Communications: from theory to practice*. Cambridge University Press, 2011.

[23] S. Shao, A. Khreishah, M. Ayyash, M. B. Rahaim, H. Elgala, V. Jungnickel, D. Schulz, T. D. Little, J. Hilt, and R. Freund, "Design and analysis of a visible-light-communication enhanced WiFi system," *IEEE J. Opt. Commun. Netw.*, vol. 7, no. 10, pp. 960–973, 2015.

[24] A. Jovicic, J. Li, and T. Richardson, "Visible light communication: opportunities, challenges and the path to market," *IEEE Commun. Mag.*, vol. 51, no. 12, pp. 26–32, 2013.

[25] P. Hu, P. H. Pathak, A. K. Das, Z. Yang, and P. Mohapatra, "PLiFi: hybrid WiFi-VLC networking using power lines," in *Proceedings of the 3rd Workshop on Visible Light Communication Systems*. ACM, 2016, pp. 31–36.

[26] A. M. Tonello and F. Versolatto, "Bottom-up statistical PLC channel modeling—Part I: Random topology model and efficient transfer function computation," *IEEE Trans. Power Del.*, vol. 26, no. 2, pp. 891–898, 2011.

[27] ——, "Bottom-up statistical PLC channel modeling—Part II: inferring the statistics," *IEEE Trans. Power Del.*, vol. 25, no. 4, pp. 2356–2363, 2010.

[28] G. Marrocco, D. Statovci, and S. Trautmann, "A PLC broadband channel simulator for indoor communications," in *IEEE International Symposium on Power Line Communications and Its Applications (ISPLC)*, 2013, pp. 321–326.

[29] D. Benyoucef, "A new statistical model of the noise power density spectrum for powerline communication," in *International Symposium on Power Line Communications and Its Applications (ISPLC), Kyoto, Japan*, 2003, pp. 136–141.

[30] IEEE Std 1901-2010, "IEEE standard for broadband over power line networks: medium access control and physical layer specifications," 2010.

[31] M. Zimmermann and K. Dostert, "Analysis and modeling of impulsive noise in broadband powerline communications," *IEEE Trans. Electromagn. Compat.*, vol. 44, no. 1, pp. 249–258, 2002.

[32] L. Di Bert, P. Caldera, D. Schwingshackl, and A. M. Tonello, "On noise modeling for power line communications," in *IEEE International Symposium on Power Line Communications and Its Applications (ISPLC)*, 2011, pp. 283–288.

[33] G. Prasad, H. Ma, M. Rahman, F. Aalamifar, and L. Lampe, *A Cumulative Power Line Noise Generator*, accessed on Dec. 25, 2016. [Online]. Available: http://www.ece.ubc.ca/~gauthamp/PLCnoise

[34] J. Grubor, S. Randel, K.-D. Langer, and J. W. Walewski, "Broadband information broadcasting using LED-based interior lighting," *J. Lightw. Technol.*, vol. 26, no. 24, pp. 3883–3892, 2008.

[35] F. R. Gfeller and U. Bapst, "Wireless in-house data communication via diffuse infrared radiation," *Proc. IEEE*, vol. 67, no. 11, pp. 1474–1486, 1979.

[36] F. J. Lo, R. Pe *et al.*, "Ray-tracing algorithms for fast calculation of the channel impulse response on diffuse IR wireless indoor channels," *Optical Engineering*, vol. 39, no. 10, pp. 2775–2780, 2000.

[37] H. Ma, *Indoor VLC ray-tracing*, accessed on Mar. 10, 2016. [Online]. Available: https://github.com/mhrex/Indoor_VLC_Ray_Tracing.git

[38] L. Grobe and K.-D. Langer, "Block-based PAM with frequency domain equalization in visible light communications," in *IEEE Globecom Workshops*, 2013, pp. 1070–1075.

[39] S. D. Personick, "Receiver design for digital fiber optic communication systems, Part I and II," *Bell system technical journal*, vol. 52, pp. 843–886, 1973.

[40] J. Armstrong and A. Lowery, "Power efficient optical OFDM," *IET Electronics Letters*, vol. 42, no. 6, pp. 370–372, 2006.

[41] J. Armstrong and B. J. Schmidt, "Comparison of asymmetrically clipped optical OFDM and DC-biased optical OFDM in AWGN," *IEEE Commun. Lett.*, vol. 12, no. 5, pp. 343–345, 2008.

[42] H. Elgala, R. Mesleh, and H. Haas, "An LED model for intensity-modulated optical communication systems," *IEEE Photon. Technol. Lett.*, vol. 22, no. 11, pp. 835–837, 2010.

[43] S. D. Dimitrov, "Analysis of OFDM-based intensity modulation techniques for optical wireless communications," Ph.D. dissertation, University of Edinburgh, Jul. 2013.

[44] J. J. Bussgang, "Crosscorrelation functions of amplitude-distorted Gaussian signals," *Technical report, MIT Research Laboratory of Electronics*, 1952.

[45] D. Dardari, V. Tralli, and A. Vaccari, "A theoretical characterization of nonlinear distortion effects in OFDM systems," *IEEE Trans. Commun.*, vol. 48, no. 10, pp. 1755–1764, 2000.

[46] S. Randel, F. Breyer, S. C. Lee, and J. W. Walewski, "Advanced modulation schemes for short-range optical communications," *IEEE J. Sel. Topics Quantum Electron.*, vol. 16, no. 5, pp. 1280–1289, 2010.

[47] J. N. Laneman, D. N. Tse, and G. W. Wornell, "Cooperative diversity in wireless networks: Efficient protocols and outage behavior," *IEEE Trans. Inf. Theory*, no. 12, pp. 3062–3080, 2004.

[48] E. W. Weisstein, "Heaviside step function," *From MathWorld–A Wolfram Web Resource. http://mathworld. wolfram. com/HeavisideStepFunction.html*, 2008.

[49] C. Wengerter, J. Ohlhorst, V. Elbwart, and A. G. Edler, "Fairness and throughput analysis for generalized proportional fair frequency scheduling in OFDMA," in *IEEE 61st Vehicular Technology Conference*, vol. 3, 2005, pp. 1903–1907.

[50] J. Kennington and Z. Wang, "A shortest augmenting path algorithm for the semi-assignment problem," *Operations Research*, vol. 40, no. 1, pp. 178–187, 1992.

[51] J. Lofberg, "YALMIP: A toolbox for modeling and optimization in MATLAB," in *IEEE International Symposium on Computer Aided Control Systems Design*, 2004, pp. 284–289.

[52] "MOSEK," http://docs.mosek.com/7.0/toolbox/, accessed: 2016-03-01.

[53] A. M. Frieze, "A bilinear programming formulation of the 3-dimensional assignment problem," *Mathematical Programming*, vol. 7, no. 1, pp. 376–379, 1974.

[54] H. W. Kuhn, "The Hungarian method for the assignment problem," *Naval research logistics quarterly*, vol. 2, no. 1-2, pp. 83–97, 1955.

[55] J. Munkres, "Algorithms for the assignment and transportation problems," *Journal of the Society for Industrial & Applied Mathematics*, vol. 5, no. 1, pp. 32–38, 1957.

[56] Y. Liu and M. Tao, "Optimal channel and relay assignment in OFDM-based multi-relay multi-pair two-way communication networks," *IEEE Trans. Commun.*, vol. 60, no. 2, pp. 317–321, 2012.

[57] Luxeon, http://www.luxeonstar.com/white-3985k-20mm-star-coolbase-led-190lm, [Online; accessed 10-Feb-2016].

[58] H. A. Latchman, S. Katar, L. Yonge, and S. Gavette, *Homeplug AV and IEEE 1901: A Handbook for PLC Designers and Users*. John Wiley & Sons, 2013.

[59] T. Esmailian, F. R. Kschischang, and P. Glenn Gulak, "In-building power lines as high-speed communication channels: channel characterization and a test channel ensemble," *International Journal of Communication Systems*, vol. 16, no. 5, pp. 381–400, 2003.

[60] J. A. Cortés, L. Diez, F. J. Cañete, and J. J. Sánchez-Martínez, "Analysis of the indoor broadband power-line noise scenario," *IEEE Trans. Electromagn. Compat.*, vol. 52, no. 4, pp. 849–858, 2010.

[61] H. Le Minh, Z. Ghassemlooy, D. O'Brien, and G. Faulkner, "Indoor gigabit optical wireless communications: challenges and possibilities,"

in *12th International Conference on Transparent Optical Networks (ICTON)*, 2010.

[62] M. Tunc, E. Perrins, and L. Lampe, "Optimal LPTV-aware bit loading in broadband PLC," *IEEE Trans. Commun.*, vol. 61, no. 12, pp. 5152–5162, 2013.